# Hyperfine structure of the metastable $^3P_2$ state of alkaline-earth-metal atoms as an accurate probe of nuclear magnetic octupole moments

K. Beloy and A. Dereviako
*Physics Department, University of Nevada, Reno, Nevada 89557, USA*

W. R. Johnson
*Physics Department, University of Notre Dame, Notre Dame, Indiana 46566, USA*
(Received 13 September 2007; published 25 January 2008)

Measuring the hyperfine structure (HFS) of long-lived $^3P_2$ states of divalent atoms may offer the opportunity of extracting relatively unexplored nuclear magnetic octupole and electric hexadecapole moments. Here, using relativistic many-body methods of atomic structure and the nuclear shell model, we evaluate the effect of these higher nuclear moments on the hyperfine structure. We find that the sensitivity of HFS interval measurements in $^{87}$Sr needed to reveal the perturbation caused by the nuclear octupole moment is on the order of kHz. The results of similar analyses for $^9$Be, $^{25}$Mg, and $^{43}$Ca are also reported.

## I. INTRODUCTION

Progress in cooling and trapping techniques has enabled a number of advances in precision measurements of atomic properties. Compared to more traditional beam spectroscopy, trapping atoms or ions increases interrogation times and enhances spectral resolution. This is a well-recognized experimental trend spanning from the searches for permanent electric-dipole moments to atomic clocks. Here, we point out that measuring the hyperfine structure of long-lived $^3P_2$ states of cold divalent atoms may facilitate extracting the so far relatively unexplored nuclear magnetic octupole moments.

A nucleus may be described as a collection of electromagnetic moments. Generally, a nucleus of spin $I$ possesses $2I$ moments beyond the monopole. Most well known are the magnetic dipole $(\mu)$ and the electric quadrupole $(Q)$ moments. These two leading moments have been studied extensively and have contributed to the understanding of nuclear forces. For example, discovery of the quadrupole moment of the deuteron led to introducing nuclear tensor forces [1]. Here, we are interested in the next two moments in the multipolar hierarchy: nuclear magnetic octupole $(\Omega)$ and electric hexadecapole $(\Pi)$ moments.

Electromagnetic fields of various nuclear moments perturb the motion of atomic electrons and reveal themselves in the hyperfine structure (HFS) of atomic and molecular levels. The resulting hyperfine intervals are conventionally parametrized in terms of the HFS constants $A, B, C, D, \ldots$, each being proportional to the relevant nuclear multipolar moment. The perturbation becomes weaker as the rank of the multipole moment increases, and detecting the influence of higher multipole moments on the HFS intervals requires increasingly longer interrogation times. Also, to observe the effects of higher rank multipoles on the HFS structure one is forced to work with electronic states of relatively high angular momenta $J$ since the $2^k$-pole moment only contributes in first order to the HFS structure of levels with $J \geq k/2$. These two factors have limited the determination of the octupole HFS constants to a small number of isotopes of Cl [2], Ga

[3], Br [4], In [5], V [6], Eu [7], Lu [8], and Hf [9]. All of the above measurements have been carried out either on the ground state or on metastable states. The most recent octupole moment measurement was carried on the short-lived $6p_{3/2}$ state of $^{133}$Cs [10]. Except for the case of the monovalent Cs atom, deducing octupole moments from measured HFS constants presents a formidable challenge, owing to the fact that the prerequisite atomic-structure calculations become inaccurate for multivalent atoms. As a result, previous analyses focused primarily on *ratios* of octupole moments for various isotopes of the same atom, because the atomic-structure factor cancels out when ratios of HFS constants are formed. By contrast, the divalent alkaline-earth-metal atoms considered here potentially yield direct values of the nuclear octupole moments.

$^3P_2$ states in alkaline-earth-metal atoms are well suited for extracting nuclear magnetic octupole moments. We list the relevant isotopes in Table I. The atomic lifetimes are longer than 100 s and are long enough to allow for a sufficiently high spectral resolution. Moreover, successful trapping of the $^3P_2$ alkaline-earth-metal atoms Sr and Ca has been recently reported in a number of laboratories and there are ongoing efforts with Mg [13–16]. A typical trapping time is longer than 10 s. Since the magnetic trap perturbs the atomic level structure, a plausible experiment could involve microwave spectroscopy of freely falling atoms when trapping fields are turned off. Even then, the interrogation time is sufficiently long to permit a determination of the magnetic octupole HFS constant. To extract the nuclear octupole moment from the measured HFS constant, one requires electronic-structure calculations. As shown in this paper, such supporting calculations can be carried out with an accuracy of a few percent.

This paper is organized as follows. In Sec. II we recapitulate the major results from the relativistic theory of the hyperfine interaction. The consideration includes first-order effects of nuclear dipole, quadrupole, octupole, and hexadecapole moments and second-order dipole-dipole and dipole-quadrupole effects. In Sec. III, we focus on the electronic-structure aspects of the problem and evaluate electronic coupling constants using a configuration-interaction

TABLE I. Nuclear parameters and lifetimes of the $^3P_2$ states of the stable isotopes of Be, Mg, Ca, and Sr. $I$ is the nuclear spin; the superscript $\pi$ represents the parity. Experimental dipole and quadrupole values are from Ref. [11]. Octupole and hexadecapole values are from a single-particle approximation (see Appendix A). Lifetimes for the $^3P_2$ states are from Ref. [12].

| Isotope | $I^\pi$ | $\mu^{\exp}(\mu_N)$ | $Q^{\exp}$ (b) | $\Omega^{\rm sp}({\rm b}\times\mu_N)$ | $\Pi^{\rm sp}$ (b$^2$) | $^3P_2$ lifetime (s) |
|---------|---------|---------------------|----------------|---------------------------------------|------------------------|----------------------|
| $^9$Be | $3/2^-$ | $-1.177492(17)$ | $+0.053(3)$ | $-0.073$ | $0.00$ | |
| $^{25}$Mg | $5/2^+$ | $-0.85545(8)$ | $+0.201(3)$ | $-0.15$ | $0.00$ | $1.06\times10^3$ |
| $^{43}$Ca | $7/2^-$ | $-1.317643(7)$ | $-0.049(5)$ | $-0.23$ | $0.00$ | $5.13\times10^2$ |
| $^{87}$Sr | $9/2^+$ | $-1.0936030(13)$ | $+0.335(20)$ | $-0.38$ | $0.00$ | $1.29\times10^2$ |

(CI) method coupled with many-body perturbation theory (MBPT). We refer to this approximation as the CI+MBPT method. Further, in Sec. IV, we discuss our results for the HFS of the $^3P_2$ level in $^{87}$Sr. Results for isotopes of Be, Mg, and Ca are tabulated in Appendix C. Finally, conclusions are drawn in Sec. V. The paper also has several appendices where we tabulate results of a technical nature. Unless specified otherwise, atomic units $\hbar=|e|=m_e=1$, and Gaussian electromagnetic units are employed throughout.

## II. NUCLEAR MOMENTS AND THE HYPERFINE INTERACTION

The electric and vector potential of a nucleus modeled as a collection of pointlike multipole moments may be expressed as

$$\varphi(\mathbf{r}) = \sum_{k,\mu}(-1)^\mu \frac{1}{r^{k+1}}C_{k,\mu}(\hat{\mathbf{r}})\mathcal{Q}_{k,-\mu},$$

$$\mathbf{A}(\mathbf{r}) = -i\sum_{k,\mu}(-1)^\mu \frac{1}{r^{k+1}}\sqrt{\frac{k+1}{k}}\mathbf{C}_{k,\mu}^{(0)}(\hat{\mathbf{r}})\mathcal{M}_{k,-\mu}, \quad (1)$$

where $C_{k,\mu}$ and $\mathbf{C}_{k,\mu}^{(0)}$ are normalized spherical harmonics and vector spherical harmonics, respectively (see, for example, Ref. [17]). In these expressions, $\mathcal{Q}_{k,\mu}$ and $\mathcal{M}_{k,\mu}$ are components of the nuclear electric and magnetic $2^k$-pole (MJ and EJ) moment operators, respectively. Each of the moments is an irreducible tensor operator of rank $k$. Parity and time-reversal symmetries require that $k$ is even for the electric moments and $k$ is odd for the magnetic moments. Components of these tensors are conventionally parametrized using $c$ numbers that are defined as expectation values of the zero components of the operators in a nuclear stretched state $|I,M_I=I\rangle$. We will employ the following notation for the "stretched" matrix element of a tensor operator $O_{k,\mu}$:

$$\langle O_k\rangle_I \equiv \langle I, M_I = I|O_{k,0}|I, M_I = I\rangle.$$

In particular, the magnetic-dipole, electric-quadrupole, magnetic-octupole, and electric-hexadecapole moments of the nucleus are defined as

$$\mu = \langle \mathcal{M}_1\rangle_I,$$

$$Q = 2\langle \mathcal{Q}_2\rangle_I,$$

$$\Omega = -\langle \mathcal{M}_3\rangle_I,$$

$$\Pi = \langle \mathcal{Q}_4\rangle_I.$$

The stretched matrix elements are related to the reduced matrix elements by

$$\langle I\|O_k\|I\rangle \equiv \begin{pmatrix} I & k & I \\ -I & 0 & I \end{pmatrix}^{-1}\langle O_k\rangle_I.$$

The interaction Hamiltonian for a single electron in an electromagnetic field is given by

$$h_{\rm em}(\mathbf{r}) = \alpha\cdot\mathbf{A}(\mathbf{r}) - \varphi(\mathbf{r}),$$

and the total electromagnetic interaction Hamiltonian is then given by

$$H_{\rm em} = \sum_i h_{\rm em}(\mathbf{r}_i),$$

where the sum runs over all electron coordinates. Substituting the multipolar expansions (1) into the electromagnetic interaction Hamiltonian, we arrive at an expression for rotationally invariant hyperfine interaction (HFI) Hamiltonian in the form of

$$H_{\rm HFI} = \sum_{k,\mu}(-1)^\mu T_{k,\mu}^e T_{k,-\mu}^n.$$

Here the spherical tensors (of rank $k$) $T_{k,\mu}^e$ act on electronic coordinates and $T_{k,\mu}^n$ operate in the nuclear space. We identify $T_{k,\mu}^n \equiv \mathcal{M}_{k,\mu}$ for odd $k$ and $T_{k,\mu}^n \equiv \mathcal{Q}_{k,\mu}$ for even $k$. Explicitly, electronic tensors read

$$T_{k,\mu}^e = \sum_i t_{k,\mu}^e(\mathbf{r}_i),$$

with

$$t_{k,\mu}^e(\mathbf{r}) = \begin{cases} -\dfrac{1}{r^{k+1}}C_{k,\mu}(\hat{\mathbf{r}}) & \text{electric (even } k), \\[2ex] -\dfrac{i}{r^{k+1}}\sqrt{\dfrac{k+1}{k}}\alpha\cdot\mathbf{C}_{k,\mu}^{(0)}(\hat{\mathbf{r}}) & \text{magnetic (odd } k). \end{cases}$$

$$(2)$$

Matrix elements of these operators for Dirac bispinors are listed in Appendix B.

Now we recapitulate the application of perturbation theory to determining the hyperfine structure of atomic lev-

els. In the presence of the multipolar fields produced by the nucleus, the total electronic angular momentum $\mathbf{J}$ is no longer conserved. The conserved angular momentum includes the nuclear angular momentum $\mathbf{I}$; explicitly this conserved angular momentum is $\mathbf{F}=\mathbf{I}+\mathbf{J}$. The proper basis consists of states $|\gamma IJFM_F\rangle$ generated by coupling nuclear and electronic wave functions,

$$|\gamma IJFM_F\rangle = \sum_{M_J, M_I} C_{JM_J;IM_I}^{FM_F} |\gamma JM_J\rangle |IM_I\rangle,$$

with $\gamma$ encapsulating the remaining electronic quantum numbers and the coupling coefficients being the conventional Clebsch-Gordon coefficients. For fixed values of $J$ and $I$, the values of $F$ range in $|J-I|\le F\le J+I$, implying that an unperturbed level with angular momentum $J$ is split into $2J+1$ levels for $J<I$ and into $2I+1$ levels otherwise.

A matrix element of the HFI in the coupled basis is

$$\langle \gamma' IJ'F'M_F'|H_{\mathrm{HFI}}|\gamma IJFM_F\rangle$$
$$= \delta_{F'F}\delta_{M_F'M_F}$$
$$\times(-1)^{I+J+F}\sum_k \begin{Bmatrix} F & J & I \\ k & I & J' \end{Bmatrix} \langle \gamma'J'||T_k^e||\gamma J\rangle\langle I||T_k^n||I\rangle, \quad (3)$$

the $\delta$ symbols reflecting the scalar character of the HFI in the coupled basis. Hyperfine corrections to an unperturbed level are given to first order by the diagonal matrix elements of $H_{\mathrm{HFI}}$. For convenience, we write this correction in terms of the $F$-independent product of the stretched matrix elements

$$W_F^{(1)} = \langle \gamma IJFM_F|H_{\mathrm{HFI}}|\gamma IJFM_F\rangle = \sum_k X_k(IJF)\langle T_k^e\rangle_J\langle T_k^n\rangle_I,$$

with

$$X_k(IJF) = (-1)^{I+J+F}\frac{\begin{Bmatrix} F & J & I \\ k & I & J \end{Bmatrix}}{\begin{pmatrix} J & k & J \\ -J & 0 & J \end{pmatrix}\begin{pmatrix} I & k & I \\ -I & 0 & I \end{pmatrix}}.$$

The first-order $F$-dependent effects are conventionally parametrized in terms of the hyperfine structure constants $A, B, C, D, \ldots$. Successive labels correspond to contributions of a multipole of increasing multipolarity, e.g., $A$ is due to the magnetic dipole moment, $B$ is due to the electric quadrupole moment, etc. The constants, up to $D$, are defined as in [18]

$$A = \frac{1}{IJ}\langle T_1^n\rangle_I\langle T_1^e\rangle_J = \frac{1}{IJ}\mu\langle T_1^e\rangle_J,$$

$$B = 4(\langle T_2^n\rangle_I\langle T_2^e\rangle_J) = 2(Q\langle T_2^e\rangle_J),$$

$$C = \langle T_3^n\rangle_I\langle T_3^e\rangle_J = -\Omega\langle T_3^e\rangle_J,$$

$$D = \langle T_4^n\rangle_I\langle T_4^e\rangle_J = \Pi\langle T_4^e\rangle_J. \quad (4)$$

The second-order (in the HFI) correction for the state described by electronic quantum numbers $\gamma$ and $J$ is

$$W_F^{(2)} = \sum_{\gamma'J'} \frac{|\langle \gamma'IJ'FM_F|H_{\mathrm{HFI}}|\gamma IJFM_F\rangle|^2}{E_{\gamma J}-E_{\gamma'J'}},$$

where the sum excludes the case $(\gamma'J')=(\gamma J)$. With Eq. (3) this can be expressed explicitly in terms of reduced matrix elements as

$$W_F^{(2)} = \sum_{\gamma'J'}\frac{1}{E_{\gamma J}-E_{\gamma'J'}}\sum_{k_1,k_2}\begin{Bmatrix} F & J & I \\ k_1 & I & J' \end{Bmatrix}\begin{Bmatrix} F & J & I \\ k_2 & I & J' \end{Bmatrix}$$
$$\times\langle \gamma'J'||T_{k_1}^e||\gamma J\rangle\langle \gamma'J'||T_{k_2}^e||\gamma J\rangle\langle I||T_{k_1}^n||I\rangle\langle I||T_{k_2}^n||I\rangle.$$

For the case of interest, where $J=2$, the sum over $(\gamma'J')$ is dominated by contributions from the adjacent fine structure levels $(\gamma 1)$ and the sum over $k_1k_2$ is dominated by the dipole-dipole $(k_1=k_2=1)$ term. If we limit ourselves to the dipole-dipole and dipole-quadrupole terms, then we may express the second-order correction as

$$W_F^{(2)} = \left|\begin{Bmatrix} F & J & I \\ 1 & I & J-1 \end{Bmatrix}\right|^2\eta + \begin{Bmatrix} F & J & I \\ 1 & I & J-1 \end{Bmatrix}$$
$$\times\begin{Bmatrix} F & J & I \\ 2 & I & J-1 \end{Bmatrix}\zeta$$

where $\eta$ and $\zeta$ are $F$-independent terms given by

$$\eta = \frac{(I+1)(2I+1)}{I}\mu^2\frac{|\langle \gamma J-1||T_1^e||\gamma J\rangle|^2}{E_{\gamma J}-E_{\gamma J-1}}, \quad (5)$$

$$\zeta = \frac{(I+1)(2I+1)}{I}\sqrt{\frac{2I+3}{2I-1}}$$
$$\times\mu Q\frac{\langle \gamma J-1||T_1^e||\gamma J\rangle\langle \gamma J-1||T_2^e||\gamma J\rangle}{E_{\gamma J}-E_{\gamma J-1}}. \quad (6)$$

In the above expressions, $\gamma$ denotes a given fine structure term such as $^3P_2$ and that $J'=J-1=1$.

## III. CI+MBPT ELECTRONIC WAVE FUNCTIONS

A precise analysis of the hyperfine structure depends on accurate electronic wave functions as well as nuclear multipole moments. To obtain accurate electronic wave functions, we used a combined method of configuration interaction (CI) and many-body perturbation theory (MBPT), which we refer to as CI+MBPT. The CI+MBPT method is described in detail, for example, in Refs. [19,20]. Here, we restrict the presentation to a qualitative discussion and then apply the CI+MBPT method to determination of the HFS couplings.

The accuracy of the CI method is limited only by the completeness of the set of configurations used. In the context of CI+MBPT we refer to the subspace containing the configurations to be treated by the CI method as the model space. In CI+MBPT, additional contributions from configurations which are not in the model space can be accounted for by MBPT. For our purposes, we are interested in finding accurate wave functions. It is worth noting that the wave functions determined by the CI+MBPT analysis lie completely within the model space.

In deciding which configurations are to be included in the model space, we consider two things. First, configurations which interact strongly with the configuration of interest must be included in the model space. The main purpose here is to expand the model space to a degree in which the wave function can be described accurately. Second, configurations with energies which are nearly degenerate with the configuration of interest should also be included in the model space. These configurations lead to convergence problems in MBPT and are treated nonperturbatively by the CI method. Of course, "strongly" and "nearly degenerate" are relative terms which depend on the level of accuracy desired.

For the alkaline-earth-metal systems considered in this paper, we start with a lowest-order description of our system as two valence electrons outside a closed core in a central field. Configurations involving different excitations of the valence electrons outside the closed core tend to interact strongly and have relatively close energies. These configurations compose our model space. Additional contributions from configurations involving excitations from core electrons are then accounted for within the framework of MBPT.

The relevant diagrams are shown in Fig. 1. The Coulomb interaction between the two valence electrons is taken into account essentially to all orders of perturbation theory and the remaining many-body effects (involving core excitations in the intermediate state) are treated in the second order of MBPT. In Fig. 1 the single-particle states are assumed to be generated in the frozen-core ($V^{N-2}$) Dirac-Hartree-Fock (DHF) approximation where the so-called one-body (loop) diagrams vanish identically.

The specific approach that we used here is somewhat more sophisticated [20]: as the single-particle orbitals we employ the so-called Brueckner orbitals. This approach incorporates the diagrams Fig. 1(b) from the onset and also subsumes higher-order chains. Then the single-particle states (vertical lines) in the remaining diagrams are replaced by the Brueckner orbitals. The entire scheme incorporates all the second-order MBPT effects and includes certain classes of diagrams to all orders. Technically, generating Brueckner orbitals requires an energy-dependent self-energy operator (see, e.g., Ref. [20]) $\Sigma(\varepsilon_\kappa)$, which generally leads to nonor-
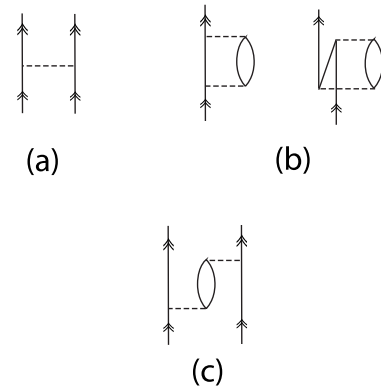


FIG. 1. Sample Brueckner-Goldstone diagrams included in the effective CI+MBPT Hamiltonian. (a) Coulomb interaction between the two valence electrons. The double arrows indicate that the single-particle states originate or terminate in the model space. (b) Brueckner (core-polarization) diagrams. (c) Screening diagrams.

thogonal basis sets. We avoid this problem by fixing $\varepsilon_\kappa$ to the $V^{N-2}$ DHF energy of the lowest-energy valence orbital for a given angular symmetry $\kappa$ ($\kappa$ is defined explicitly in Appendix B).

To illustrate the predictive capabilities of the CI+MBPT method, in Table II we compare the theoretical energy values with the experimental values for Sr. The difference does not exceed a few 100 cm$^{-1}$ for all the calculated energy levels. While the accuracy can be improved further, this level is sufficient for the goals of the present paper.

Solving the CI+MBPT problem reduces to diagonalizing the effective Hamiltonian in the model space. With the CI+MBPT wave functions we proceed to evaluating matrix elements. Details are given in Ref. [20]; the method builds upon the formalism originally developed for He-like systems [21]. We also include an important chain of diagrams of the random-phase approximation (RPA) in the evaluation of matrix elements. Qualitatively, RPA accounts for screening of externally applied fields (in our particular case these are the multipolar nuclear fields) by the core electrons.

Numerically, the calculations were carried out using $B$-spline basis sets. It is worth mentioning our modification

TABLE II. Energies of Sr I obtained from CI+MBPT are compared to experimental values. The table is partitioned into states of definite $J$ and parity. Energies are referenced from the ground $5s^2\ ^1S_0$ state. All energy values are in cm$^{-1}$.

| $J$ | Parity | Level | | CI+MBPT | Experimental | Differential |
|-----|--------|-------|------|---------|--------------|--------------|
| 0 | even | $5s6s$ | $^1S_0$ | 30766 | 30592 | 174 |
| | | $5p^2$ | $^3P_0$ | 35798 | 35193 | 605 |
| | | $5p^2$ | $^1S_0$ | 37553 | 37160 | 393 |
| 1 | odd | $5s5p$ | $^3P_1$ | 14841 | 14504 | 337 |
| | | $5s5p$ | $^1P_1$ | 21818 | 21699 | 119 |
| | | $5s6p$ | $^3P_1$ | 34062 | 33868 | 194 |
| | | $5s6p$ | $^1P_1$ | 34293 | 34098 | 195 |
| 2 | odd | $5s5p$ | $^3P_2$ | 15212 | 14899 | 313 |
| | | $4d5p$ | $^3F_2$ | 33836 | 33267 | 569 |
| | | $4d5p$ | $^1D_2$ | 34149 | 33827 | 322 |

to the original scheme [22] of generating the orbital sets. In that scheme, boundary conditions are imposed on the small and large components of the wave function, which were found to effectively dispense of spurious states in the orbital sets (more accurately, these spurious states were shifted toward the end of the spectrum). The disadvantage that follows is that the resulting wave functions are not highly accurate near the nucleus, leading to inaccuracies in the HFI integrals of Appendix B. To remedy this problem, we followed the prescription for creating a dual kinetic-balance (DKB) basis set, as introduced by Shabaev *et al.* [23]. The DKB basis set is devoid of the problem of spurious states and capable of accurately representing the wave functions near the nucleus. The specific formulas used here for generating DHF orbital sets with a DKB basis set derived from *B* splines are presented in Ref. [24].

Another technical issue is the appearance of "intruder" states in screening diagrams, Fig. 1(c). Intermediate states (the diagram is cut across horizontally) there involve core-excited states. Since our model (CI) space is essentially complete, such core-excited states become embedded in the two-particle energy spectrum of the lowest-order model Hamiltonian. This leads to singular energy denominators in the diagrams Fig. 1(c). We remedied this problem by evaluating screening corrections only to the two-particle states that had energies below the lowest-energy core excitation. For a typical basis set the resulting subspace involved roughly 10% of the entire model space. Arguably, this prescription recovers most of the relevant correction since this low-energy subspace contains the dominant configurations.

## IV. HYPERFINE STRUCTURE OF $^{87}$Sr

Using the techniques described in the previous sections, we consider as a specific example the hyperfine structure of the lowest-energy $^3P_2$ level of $^{87}$Sr.

### A. Extracting the magnetic-octupole constant from measurement of hyperfine intervals

The nuclear spin of the stable $^{87}$Sr isotope is $I=9/2$, and so there are five hyperfine structure levels $F=5/2,\ldots,13/2$. First-order corrections are then characterized by four hyperfine structure constants $A$, $B$, $C$, and $D$. In addition, the second-order dipole-dipole interaction, characterized by $\eta$, and the dipole-quadrupole interaction, characterized by $\zeta$, mix the $^3P_2$ state with the nearby fine structure $^3P_1$ state. Using the expressions given in Sec. II, we may write the hyperfine correction for $^{87}$Sr in terms of these constants as

$$W_{5/2} = -11A + \frac{11}{24}B - \frac{143}{42}C + \frac{143}{18}D,$$

$$W_{7/2} = -\frac{15}{2}A + \frac{1}{48}B + \frac{65}{21}C - \frac{52}{3}D + \frac{7\eta}{900} - \frac{7\zeta}{300\sqrt{6}},$$

$$W_{9/2} = -3A - \frac{7}{24}B + \frac{13}{6}C + \frac{91}{6}D + \frac{32\eta}{2475} - \frac{4\zeta}{825}\sqrt{\frac{2}{3}},$$

$$W_{11/2} = \frac{5}{2}A - \frac{7}{24}B - \frac{10}{3}C - \frac{56}{9}D + \frac{13\eta}{1100} + \frac{13\zeta}{550\sqrt{6}},$$

$$W_{13/2} = 9A + \frac{1}{4}B + C + D.$$

The resulting HFS intervals $\delta W_F = W_F - W_{F+1}$ are given in terms of the hyperfine constants as

$$\delta W_{5/2} = -\frac{7}{2}A + \frac{7}{16}B - \frac{13}{2}C + \frac{455}{18}D - \frac{7\eta}{900} + \frac{7\zeta}{300\sqrt{6}},$$

$$\delta W_{7/2} = -\frac{9}{2}A + \frac{5}{16}B + \frac{13}{14}C - \frac{65}{2}D - \frac{17\eta}{3300} - \frac{\zeta}{220}\sqrt{\frac{3}{2}},$$

$$\delta W_{9/2} = -\frac{11}{2}A + \frac{11}{2}C + \frac{385}{18}D + \frac{\eta}{900} - \frac{\zeta}{30\sqrt{6}},$$

$$\delta W_{11/2} = -\frac{13}{2}A - \frac{13}{24}B - \frac{13}{3}C - \frac{65}{9}D + \frac{13\eta}{1100} + \frac{13\zeta}{550\sqrt{6}}.$$

(7)

Similar expressions for the hyperfine intervals in $^3P_2$ states of stable isotopes of other alkaline-earth-metal atoms are given in Appendix C. Solving Eqs. (7) for the hyperfine constants $C$ and $D$, one finds

$$C = -\frac{3}{50}\delta W_{5/2} + \frac{7}{550}\delta W_{7/2} + \frac{21}{275}\delta W_{9/2} - \frac{147}{3575}\delta W_{11/2}$$
$$+ \frac{7\zeta}{1375\sqrt{6}},$$

(8)

$$D = \frac{3}{350}\delta W_{5/2} - \frac{9}{550}\delta W_{7/2} + \frac{3}{275}\delta W_{9/2} - \frac{9}{3575}\delta W_{11/2}.$$

(9)

Expressions for the HFS constants $C$ and $D$ in terms of hyperfine intervals for $^3P_2$ states in other isotopes of the alkaline-earth-metal atoms are given in Appendix C. The constant $C$ depends only on the second-order dipole-quadrupole interference term $\zeta$ while $D$ is independent of both $\eta$ and $\zeta$. This proposition is independent of nuclear spin $I$, as shown in Appendix D.

To reiterate, measuring hyperfine intervals of the $^3P_2$ level should allow one to deduce the magnetic-octupole HFS constant $C$, limited only by the knowledge of $\zeta$. With the aid of calculations of the electronic-structure factor presented below one may extract the nuclear magnetic-octupole moment of interest.

### B. Electronic-structure factors

From Eqs. (4) and (5) we see that the HFS constants may be written in terms of products of electronic matrix elements and nuclear multipole moments. We evaluate the electronic matrix elements using the relativistic many-body method de-

TABLE III. Breakdown of many-body corrections to hyperfine structure constants of the $^{87}$Sr $5s5p\ ^3P_2$ state. We used $\mu=-1.0936\mu_N$ and $Q=0.305(2)$ b (Ref. [25]) in tabulating $A$ and $B$ constants. The final result is compared with experimental values from Ref. [26]. CI-DHF corresponds to CI values computed using single-particle basis generated in the frozen-core ($V^{N-2}$) DHF potential.

| | $A$, MHz | $B$, MHz | $C/\Omega$, MHz/($\mu_N \times$ b) | $D/\Pi$, MHz/b$^2$ |
|---|---|---|---|---|
| CI-DHF | −147.1 | 35.6 | $3.54 \times 10^{-4}$ | $0.54 \times 10^{-12}$ |
| | | Many-body corrections | | |
| $\Delta$ BO | −41.9 | 10.2 | $1.03 \times 10^{-4}$ | $0.85 \times 10^{-12}$ |
| $\Delta$ Screen | 0.4 | −4.6 | $-0.42 \times 10^{-4}$ | $2.71 \times 10^{-12}$ |
| $\Delta$ RPA | −42.0 | 21.0 | $1.15 \times 10^{-4}$ | $0.55 \times 10^{-12}$ |
| Final | −230.6 | 62.2 | $5.30 \times 10^{-4}$ | $4.65 \times 10^{-12}$ |
| Experiment | −212.765(1) | 67.215(15) | | |

scribed in Sec. III. We present the results of our calculations at various levels of approximation in Table III.

In generating the DHF orbitals we included nuclear-size effects by assuming a Fermi charge distribution inside the nucleus. For the computation of HFI integrals, however, we assumed a point-size nucleus. The observed effect on the choice of a particular model of nuclear distribution is below our theoretical error for solving the electronic-structure problem.

There are several observations to be made with respect to the many-body calculations. First of all, we find that for Sr, the configuration $5p_{3/2}5s_{1/2}$ provides the dominant (92%) contribution to the CI wave function of the $^3P_2$ state. In particular, due to the angular selection rules the constants $B$ and $C$ are determined by the matrix elements involving the $5p_{3/2}$ orbital from this dominant configuration. By contrast, the dominant $5p_{3/2}5s_{1/2}$ configuration does not contribute to the electric-hexadecapole (E4) constant due to selection rules for single-particle matrix elements (see Appendix B). Therefore the E4 electronic factor is strongly suppressed, as its value is accumulated entirely due to admixed configurations.

We find that the Brueckner orbital (BO) (core-polarization) corrections universally increase the absolute value of all the constants. Qualitatively, core polarization describes an attraction of the valence electron by the core. This attraction leads to enhanced density closer to the nucleus and simultaneously larger hyperfine constants. Similarly, the computed RPA corrections show that the internal nuclear fields are enhanced by virtual core excitations. The screening diagrams, Fig. 1(c), qualitatively represent an effect of "cross talking" between electrons via core polarization: a valence electron polarizes the core and this induced polarization attracts or repels another valence electron. We see for the magnetic-dipole HFS constant that this effect is relatively weak compared to the other many-body corrections; however, its effect is more substantial for the electric-quadrupole and magnetic-octupole HFS constants. In all three of these cases, the screening contribution has the effect of decreasing the absolute value of the HFS constants.

Finally, in Table III we compare our *ab initio* results with experimental values for $A$ and $B$. We find an 8% agreement for both constants. We believe that these accuracies are in-

dicative of the theoretical error for the electronic factor entering the magnetic-octupole constant $C$. The accuracy of computing the electronic factor for the HFS constant $D$ is expected to be worse because the entire value is accumulated due to correlation effects.

We have carried out similar many-body calculations for the parameters $\eta$ and $\zeta$ entering the second-order correction to the hyperfine constants. For $^{87}$Sr, we find $\eta=6.65$ MHz and $\zeta=0.529$ MHz. These second-order corrections are scaled to the experimental $A$ and $B$ coefficients and are accurate to 2%. The second-order dipole-quadrupole contribution to $C$ is

$$\Delta C(^{87}\text{Sr}) = \frac{7\zeta}{1375\sqrt{6}} = 1.10(2)\ \text{kHz.} \qquad (10)$$

In this section we have described our calculations for $^{87}$Sr. The corresponding results for $^9$Be, $^{25}$Mg, and $^{43}$Ca are given in Appendix C.

## V. DISCUSSION

At this point we combine the computed electronic-structure factors for the magnetic-octupole constants (Tables III and IV) and the nuclear shell-model prediction for the M3 moment $\Omega$ (Table I and Appendix A). We find that

$$C(^9\text{Be}) = -3.57 \times 10^{-2}\ \text{Hz,}$$

$$C(^{25}\text{Mg}) = -2.57\ \text{Hz,}$$

$$C(^{43}\text{Ca}) = -16.2\ \text{Hz,}$$

$$C(^{87}\text{Sr}) = -201\ \text{Hz.} \qquad (11)$$

In particular, for Sr, using Eq. (8), we may deduce that an experimental sensitivity in measuring the HFS intervals on the order of $\sigma_{\delta W} \approx 1$ kHz would result in an uncertainty in the $C$ constant on the order of $\sigma_C \approx 0.11\sigma_{\delta W} \approx 100$ Hz and would thus be capable of revealing the effects of a $C$ constant of the predicted magnitude.

The expression for the constant of interest $C$ in terms of HFS splittings contains the second-order dipole-quadrupole

correction, see, e.g., Eq. (8) for Sr. If the experiment measures HFS intervals with a vanishingly small error bar, the extraction of $\Omega$ would be limited by the error in this correction. Our estimated error bar for Sr, Eq. (10) is 20 Hz, which translated into 10% error bar for $C(^{87}\mathrm{Sr})$ of predicted magnitude. A similar conclusion holds for Ca, while for Mg our estimated uncertainty in the dipole-quadrupole correction is comparable with the predicted size of $C$. For Be, our present uncertainty of 0.2 Hz in the dipole-quadrupole correction precludes clean extraction of the octupole moment. Notice, however, that the nuclear shell model estimates of the nuclear octupole moment may be unreliable. If the $^{133}\mathrm{Cs}$ experiment [10] is of any indication, the "true" size of the octupole constant may be much larger (a factor of 40) than predicted. Then the dipole-quadrupole corrections become mostly irrelevant.

We emphasize that the values (11) are only estimates based on the nuclear-shell model; measuring $C$ would show deviations from these estimates. In a particular case of $^{133}\mathrm{Cs}$, the measured and the predicted values differed by a factor of 40 [10]. It remains to be seen if such large deviations from the nuclear shell model would be revealed experimentally for the nuclei considered in the present work.

### ACKNOWLEDGMENTS

### APPENDIX A: NUCLEAR MOMENTS FROM A SINGLE-PARTICLE MODEL

A crude approximation to the nuclear moments can be achieved by representing the nucleus by a single nucleon. For even-odd (even number of protons, odd number of neutrons) nuclei we use a single neutron, and for odd-even nuclei we use a single proton. Using formulas by [27], we may write the moments in this single-particle model as

$$
\mu^{\mathrm{sp}} = \mu_N I \times
\begin{cases}
[g_l + (g_s - g_l)/2I] & \text{for } I = l + \tfrac{1}{2}, \\
[g_l - (g_s - g_l)/(2I + 2)] & \text{for } I = l - \tfrac{1}{2},
\end{cases}
$$

$$
Q^{\mathrm{sp}} = -e\langle r^2\rangle g_l \frac{2I - 1}{2I + 2},
$$

$$
\Omega^{\mathrm{sp}} = \mu_N \langle r^2\rangle \frac{3}{2} \frac{(2I - 1)}{(2I + 4)(2I + 2)}
$$
$$
\times
\begin{cases}
(I + 2)\left[\left(I - \tfrac{3}{2}\right)g_l + g_s\right] & \text{for } I = l + \tfrac{1}{2}, \\
(I - 1)\left[\left(I + \tfrac{5}{2}\right)g_l - g_s\right] & \text{for } I = l - \tfrac{1}{2},
\end{cases}
$$

$$
\Pi^{\mathrm{sp}} = -e\langle r^2\rangle g_l \frac{3}{8} \frac{(2I - 1)(2I - 3)}{(2I + 4)(2I + 2)},
$$

where $g_l = +1$, $g_s = 5.58$ for a proton and $g_l = 0$, $g_s = -3.83$ for a neutron. All of the stable isotopes considered in this paper have even-odd nuclei. This has the immediate consequence $Q^{\mathrm{sp}} = 0$ and $\Pi^{\mathrm{sp}} = 0$ for all isotopes. Furthermore, an examination of the momentum $I$ and parity $\pi$ in Table I reveals that the nucleon for each isotope must have an orbital momentum $l$ satisfying $I = l + 1/2$. With this additional consideration, $\mu^{\mathrm{sp}} = -1.92\mu_N$ for all isotopes, and the expression for the octupole moment is reduced to

$$
\Omega^{\mathrm{sp}} = \mu_N \langle r^2\rangle g_s \frac{3}{4} \frac{(2I - 1)}{(2I + 2)}.
$$

Approximating the root-mean-square value of the nuclear radii $\langle r^2\rangle^{1/2}$ as (in units of fm) 2.52, 3.05, 3.48, and 4.24 for the cases of $^9\mathrm{Be}$, $^{25}\mathrm{Mg}$, $^{43}\mathrm{Ca}$, and $^{87}\mathrm{Sr}$, respectively, yields the values for $\Omega^{\mathrm{sp}}$ given in Table I.

In the single-particle model the electromagnetic moments of the nuclei are given by the appropriate expectation values for the valence nucleon shell. In this model the even-odd nuclei would have electromagnetic moments determined by the valence neutron. In particular, since the neutron does not have an electric charge, all electric moments vanish. Certainly, the observed nonzero $Q$ moment provides information on such quantities as nuclear deformation. Similarly, an observation of the electric hexadecapole moment, which is zero in the single-particle approximation, should provide similar information on the nuclear distortion.

TABLE IV. Theoretical and experimental hyperfine structure constants for the $^3P_2$ states of $^9\mathrm{Be}$, $^{25}\mathrm{Mg}$, and $^{43}\mathrm{Ca}$. Theoretical values include the many-body effects discussed in Sec. III.

| | | $A$, MHz | $B$, MHz | $C/\Omega$, MHz/$(\mu_N \times \mathrm{b})$ | $D/\Pi$, MHz/$\mathrm{b}^2$ |
|---|---|---|---|---|---|
| $^9\mathrm{Be}$ | Theory | −119.7 | 1.43 | $4.89 \times 10^{-7}$ | |
| | Experimental[a] | −124.5368(17) | 1.429(8) | | |
| $^{25}\mathrm{Mg}$ | Theory | −127.5 | 15.8 | $1.71 \times 10^{-5}$ | $-1.39 \times 10^{-14}$ |
| | Experimental[b] | −128.445(5) | 16.009(5) | | |
| $^{43}\mathrm{Ca}$ | Theory | −179.9 | −5.50 | $7.03 \times 10^{-5}$ | $7.83 \times 10^{-13}$ |
| | Experimental[c] | −171.962(2) | −5.436(8) | | |

[a]Reference [28].
[b]Reference [29].
[c]Reference [30].

## APPENDIX B: MATRIX ELEMENTS OF THE ELECTRONIC TENSOR OPERATOR

Here we compile expressions for the matrix elements of the single-particle electronic HFI coupling operators $t^e_{k,\mu}(\mathbf{r})$ given in Eq. (2). We use the conventional parametrization of the Dirac bispinors,

$$|n\kappa m\rangle = \frac{1}{r}\begin{pmatrix} iP_{n\kappa}(r) & \Omega_{\kappa m}(\hat{r}) \\ Q_{n\kappa}(r) & \Omega_{-\kappa m}(\hat{r}) \end{pmatrix},$$

where $\kappa = (l-j)(2j+1)$ and $\Omega$ are spinor functions. With this parametrization, we find that the reduced matrix elements for the HFI couplings to electric moments of the nucleus are given by

$$\langle n'\kappa'||t^e_k||n\kappa\rangle = -\langle \kappa'||C_k||\kappa\rangle \int_0^\infty \frac{dr}{r^{k+1}}(P_{n'\kappa'}P_{n\kappa} + Q_{n'\kappa'}Q_{n\kappa}),$$

and for couplings to magnetic moments these are

$$\langle n'\kappa'||t^e_k||n\kappa\rangle = \langle \kappa'||C_k||-\kappa\rangle \left(\frac{\kappa'+\kappa}{k}\right) \int_0^\infty \frac{dr}{r^{k+1}}$$

$$\times (P_{n'\kappa'}Q_{n\kappa} + Q_{n'\kappa'}P_{n\kappa}).$$

Selection rules for these matrix elements follow from those for the matrix elements of the $C$ tensor: $|j-j'| \leq k \leq j+j'$ and the sum $l+l'$ must be even.

## APPENDIX C: HYPERFINE STRUCTURE OF THE $^3P_2$ STATE FOR $^9$Be, $^{25}$Mg, AND $^{43}$Ca

This Appendix contains a compilation of expressions relating the hyperfine intervals and the hyperfine structure constants for the $^3P_2$ states of $^9$Be, $^{25}$Mg, and $^{43}$Ca. Computed HFS constants for these isotopes, given in Table IV, are also included.

$^9$Be, $I = 3/2$:

$$\delta W_{1/2} = -\frac{3}{2}A + \frac{7}{8}B - 28C - \frac{11\eta}{600} + \frac{\sqrt{3}\zeta}{200},$$

$$\delta W_{3/2} = -\frac{5}{2}A + \frac{5}{8}B + 20C - \frac{\eta}{120} - \frac{\sqrt{3}\zeta}{40},$$

$$\delta W_{5/2} = -\frac{7}{2}A - \frac{7}{8}B - 7C + \frac{7\eta}{200} + \frac{7\zeta}{200\sqrt{3}},$$

$$C = -\frac{1}{50}\delta W_{1/2} + \frac{1}{50}\delta W_{3/2} - \frac{1}{175}\delta W_{5/2} + \frac{\zeta}{500\sqrt{3}}.$$

For $^9$Be, we find that $\eta = 25.09(4)$ MHz and $\zeta = 0.2939(2)$ MHz, leading to a value $\Delta C = 0.3394(2)$ kHz for the second-order correction to $C$.

$^{25}$Mg, $I = 5/2$:

$$\delta W_{1/2} = -\frac{3}{2}A + \frac{9}{20}B - \frac{54}{5}C + 90D - \frac{\eta}{100} + \frac{\zeta}{50\sqrt{2}},$$

$$\delta W_{3/2} = -\frac{5}{2}A + \frac{1}{2}B - 3C - 75D - \frac{13\eta}{1260} - \frac{\zeta}{210\sqrt{2}},$$

$$\delta W_{5/2} = -\frac{7}{2}A + \frac{7}{40}B + \frac{49}{5}C + 35D - \frac{\eta}{900} - \frac{11\zeta}{300\sqrt{2}},$$

$$\delta W_{7/2} = -\frac{9}{2}A - \frac{27}{40}B - \frac{27}{5}C - 9D + \frac{3\eta}{140} + \frac{33\zeta}{140\sqrt{2}},$$

$$C = -\frac{1}{30}\delta W_{1/2} - \frac{1}{70}\delta W_{3/2} + \frac{1}{20}\delta W_{5/2} - \frac{5}{252}\delta W_{7/2} + \frac{\zeta}{350\sqrt{2}},$$

$$D = \frac{1}{210}\delta W_{1/2} - \frac{3}{490}\delta W_{3/2} + \frac{3}{980}\delta W_{5/2} - \frac{1}{1764}\delta W_{7/2}.$$

For $^{25}$Mg, we find that $\eta = 5.37(1)$ MHz and $\zeta = 0.333(1)$ MHz, leading to a value $\Delta C = 0.671(2)$ kHz for the second-order correction to $C$.

$^{43}$Ca, $I = 7/2$:

$$\delta W_{3/2} = -\frac{5}{2}A + \frac{25}{56}B - \frac{55}{7}C + \frac{275}{7}D - \frac{\eta}{112} + \frac{\zeta}{112}\sqrt{\frac{5}{3}},$$

$$\delta W_{5/2} = -\frac{7}{2}A + \frac{3}{8}B - 44D - \frac{\eta}{144} - \frac{\zeta}{48\sqrt{15}},$$

$$\delta W_{7/2} = -\frac{9}{2}A + \frac{3}{56}B + \frac{48}{7}C + \frac{180}{7}D + \frac{\eta}{1680} - \frac{13\zeta}{560}\sqrt{\frac{3}{5}},$$

$$\delta W_{9/2} = -\frac{11}{2}A - \frac{33}{56}B - \frac{33}{7}C - \frac{55}{7}D + \frac{11\eta}{720} + \frac{11\zeta}{240\sqrt{15}},$$

$$C = -\frac{1}{20}\delta W_{3/2} + \frac{1}{15}\delta W_{7/2} - \frac{7}{220}\delta W_{9/2} + \frac{\zeta}{120\sqrt{15}},$$

$$D = \frac{1}{140}\delta W_{3/2} - \frac{1}{84}\delta W_{5/2} + \frac{1}{140}\delta W_{7/2} - \frac{1}{660}\delta W_{9/2}.$$

For $^{43}$Ca, we find that $\eta = 8.43(3)$ MHz and $\zeta = 0.085(1)$ MHz, leading to a value $\Delta C = -0.183(3)$ kHz for the second-order correction to $C$.

## APPENDIX D: PROOF THAT HFS CONSTANTS $C$ AND $D$ MAY BE DEFINED COMPLETELY IN TERMS OF THE HFS INTERVALS

In this section we prove that the HFS constants $C$ and $D$ can be expressed uniquely in terms of the HFS intervals even when the second-order dipole-dipole fine structure term may not be neglected. This is a nontrivial statement, as the number of linear equations for HFS intervals is less than the number of fitting parameters. For example, for $^{87}$Sr we find that there are four HFS intervals expressed in terms of five fitting parameters [see Eq. (7)].

We start by defining our HFS levels from a new energy offset $W'_F = W_F + \Delta$. The constant $\Delta$ is arbitrary and its particular choice will be shown not to affect the conclusions; consequently, a knowledge of the HFS level intervals with a convenient choice of $\Delta$ is sufficient to completely define $W'_F$ for all $F$. Including all first-order terms as well as the second-order dipole-dipole fine structure term, the levels $W'_F$ can be written as

$$W'_F = \Delta + (-1)^{I+J+F} \sum_{k'} \begin{Bmatrix} F & J & I \\ k' & I & J \end{Bmatrix} Z_{k'}$$
$$+ \left| \begin{Bmatrix} F & J & I \\ 1 & I & J-1 \end{Bmatrix} \right|^2 \eta, \tag{D1}$$

where $Z_k = \langle \gamma J \| T^e_k \| \gamma J \rangle \langle I \| T^n_k \| I \rangle$. From Eq. (4) we see that $Z_1$ is proportional to $A$, $Z_2$ is proportional to $B$, etc. The next step is to multiply every term in Eq. (D1) by $(-1)^{I+J+F}(2F+1) \begin{Bmatrix} F & J & I \\ k & I & J \end{Bmatrix}$, with $k \neq 0$, and sum over all $F$ values. Here we analyze the effect of this procedure on the individual terms of the right-hand side of Eq. (D1); to do so, we incorporate various well-known sum rules of six-$j$ symbols. The first term becomes

$$\Delta \sum_F (-1)^{I+J+F} (2F+1) \begin{Bmatrix} F & J & I \\ k & I & J \end{Bmatrix}$$
$$= \Delta \delta_{k,0} \sqrt{(2I+1)(2J+1)} = 0.$$

The second term becomes

$$\sum_{k'} Z_{k'} \sum_F (2F+1) \begin{Bmatrix} F & J & I \\ k' & I & J \end{Bmatrix} \begin{Bmatrix} F & J & I \\ k & I & J \end{Bmatrix}$$
$$= \sum_{k'} Z_{k'} \frac{\delta_{k,k'}}{(2k+1)} = \frac{1}{(2k+1)} Z_k.$$

The third term becomes

$$\eta(-1)^{2(I+J)+k+1} \sum_F (-1)^{F-I-J-k-1}(2F+1) \begin{Bmatrix} F & J & I \\ 1 & I & J-1 \end{Bmatrix}$$
$$\times \begin{Bmatrix} F & J & I \\ 1 & I & J-1 \end{Bmatrix} \begin{Bmatrix} F & J & I \\ k & I & J \end{Bmatrix}$$
$$= \eta(-1)^{2(I+J)+k+1} \begin{Bmatrix} 1 & 1 & k \\ J & J & J-1 \end{Bmatrix} \begin{Bmatrix} 1 & 1 & k \\ I & I & I \end{Bmatrix}.$$

The resulting equation may then be solved for $Z_k$, giving

$$Z_k = (2k+1) \sum_F (-1)^{I+J+F}(2F+1) \begin{Bmatrix} F & J & I \\ k & I & J \end{Bmatrix} W'_F$$
$$+ (-1)^{2(I+J)+k}(2k+1) \begin{Bmatrix} 1 & 1 & k \\ J & J & J-1 \end{Bmatrix} \begin{Bmatrix} 1 & 1 & k \\ I & I & I \end{Bmatrix} \eta.$$

First, we note that this expression does not depend on the specific choice of $\Delta$. Second, we note that for the case of $k > 2$, the triangular condition is not satisfied along the top rows of the last four six-$j$ symbols in the last expression. Since these six-$j$ symbols are then equal to zero, $Z_k$ is completely defined by the values of $W'_F$. Equivalently, we may conclude that the HFS constants $C, D, \dots$ may be expressed completely in terms of the HFS intervals, and these are the same expressions that would be obtained regardless of the inclusion of $\eta$. A more general proof can easily be given to show that with the inclusion of second-order dipole-quadrupole terms, $C$ can no longer be expressed completely in terms of the intervals, while the expression for $D$ in terms of the intervals would still remain valid (and so on to higher second-order terms if desired).

The above conclusion can also be drawn from the formulation of second-order effects as in Ref. [31], in which the second-order effects are used to describe the difference between a measured value of a HFS constant (based on first-order perturbation theory) compared to its actual value. This already assumes that all measurable HFI effects are completely described by first- and second-order perturbation theory. Further assuming that only second-order terms of the dipole-dipole type contribute to measurable effects shows that measured HFS constants differ from actual HFS constants only for the cases of constants $A$ and $B$ and not for higher constants.

[1] N. F. Ramsey, *Molecular Beams* (Oxford University Press, London, 1969).
[2] C. Schwartz, Phys. Rev. **105**, 173 (1957).
[3] R. T. Daly and J. H. Holloway, Phys. Rev. **96**, 539 (1954).
[4] H. H. Brown and J. G. King, Phys. Rev. **142**, 53 (1966).
[5] T. G. Eck and P. Kusch, Phys. Rev. **106**, 958 (1957).
[6] W. J. Childs, O. Poulsen, L. S. Goodman, and H. Crosswhite, Phys. Rev. A **19**, 168 (1979).
[7] W. J. Childs, Phys. Rev. A **44**, 1523 (1991).
[8] T. Brenner, S. Buttgenbach, W. Rupprecht, and F. Traber, Nucl. Phys. A. **440**, 407 (1985).
[9] W. G. Jin, M. Wakasugi, T. T. Inamura, T. Murayama, T. Wakui, H. Katsuragawa, T. Ariga, T. Ishizuka, and I. Sugai, Phys. Rev. A **52**, 157 (1995).
[10] V. Gerginov, A. Derevianko, and C. E. Tanner, Phys. Rev. Lett. **91**, 072501 (2003).
[11] P. Raghavan, At. Data Nucl. Data Tables **42**, 189 (1989).
[12] S. G. Porsev and A. Derevianko, Phys. Rev. A **69**, 042506 (2004).
[13] J. Grünert and A. Hemmerich, Phys. Rev. A **65**, 041401(R) (2002).
[14] S. B. Nagel, C. E. Simien, S. Laha, P. Gupta, V. S. Ashoka, and T. C. Killian, Phys. Rev. A **67**, 011401(R) (2003).
[15] X. Xu, T. H. Loftus, J. L. Hall, A. Gallagher, and J. Ye, J. Opt. Soc. Am. B **20**, 968 (2003).
[16] M. Yasuda and H. Katori, Phys. Rev. Lett. **92**, 153004 (2004).

[17] W. R. Johnson, *Atomic Structure Theory: Lectures on Atomic Physics* (Springer, New York, NY, 2007).

[18] W. Dankwort, J. Ferch, and H. Gebauer, Z. Phys. **267**, 229 (1974).

[19] V. A. Dzuba, V. V. Flambaum, and M. G. Kozlov, Phys. Rev. A **54**, 3948 (1996).

[20] I. M. Savukov and W. R. Johnson, Phys. Rev. A **65**, 042503 (2002).

[21] W. R. Johnson, D. R. Plante, and J. Sapirstein, Adv. At., Mol., Opt. Phys. **35**, 255 (1995).

[22] W. R. Johnson, S. A. Blundell, and J. Sapirstein, Phys. Rev. A **37**, 307 (1988).

[23] V. M. Shabaev, I. I. Tupitsyn, V. A. Yerokhin, G. Plunien, and G. Soff, Phys. Rev. Lett. **93**, 130405 (2004).

[24] K. Beloy and A. Derevianko, e-print arXiv:0710.3142.

[25] B. K. Sahoo, Phys. Rev. A **73**, 062501 (2006).

[26] S. M. Heider and G. O. Brink, Phys. Rev. A **16**, 1371 (1977).

[27] C. Schwartz, Phys. Rev. **97**, 380 (1955).

[28] A. Blachman and A. Lurio, Phys. Rev. **153**, 164 (1967).

[29] A. Lurio, Phys. Rev. **126**, 1768 (1962).

[30] P. Grundevik, M. Gustavsson, I. Lindgren, G. Olsson, L. Robertsson, A. Rosen, and S. Svanberg, Phys. Rev. Lett. **42**, 1528 (1979).

[31] J. L. Armstrong, *Theory of the Hyperfine Structure of Free Atoms* (Wiley-Interscience, New York, 1971).